

Marginal Densities, Factor Graph Duality, and High-Temperature Series Expansions

Mehdi Molkaeraie

mehdi.molkaeraie@alumni.ethz.ch

Abstract—We prove that the marginals densities of a primal normal factor graph and the corresponding marginal densities of its dual normal factor graph are related via local mappings. The mapping relies on no assumptions on the size, on the topology, or on the parameters of the graphical model. The mapping provides us with a simple procedure to transform simultaneously the estimated marginals from one domain to the other, which is particularly useful when such computations can be carried out more efficiently in one of the domains. In the case of the Ising model, valid configurations in the dual normal factor graph of the model coincide with the terms that appear in the high-temperature series expansion of the partition function. The subgraphs-world process (as a rapidly mixing Markov chain) can therefore be employed to draw samples according to the global probability mass function of the dual normal factor graph of ferromagnetic Ising models.

I. INTRODUCTION

In any probabilistic inference problem, we are concerned with computing marginal densities of a global multivariate distribution, which is, in general, intractable [1]. Our approach to the problem of estimating marginal densities hinges on the notions of the dual normal realization [2] and the dual normal factor graph (NFG) [3], [4]. We will use the terms marginal probability mass function (PMF) and marginal density interchangeably.

The normal factor graph duality theorem states that the partition function of a primal normal factor graph and the partition function of its dual are equal up to some known scale factor (which depends on the topology of the NFG) [3]. In this paper, our main result states that marginal densities of the global PMF of a primal NFG and of its dual NFG are also related via local mappings. The mapping is independent of the size of the model, of the topology of the graphical model, and of any assumptions on the parameters of the model. As model, we will mainly focus on binary models with pairwise (nearest-neighbor) interactions, with symmetric factors between interacting pairs, but with arbitrary topology. However, the mapping can be extended to models with more general interactions (e.g., higher-order Markov random fields) and to non-binary models.

In either domain, estimates of marginal densities can be obtained via variational inference algorithms [5] or via Monte Carlo methods [6]–[8]. We can then transform the estimates “simultaneously” from one domain the other. The mapping is practically advantageous in cases where estimating marginal densities can be done more efficiently in one domain, compared to the other. For example, there is a rapidly mixing Markov chain (called the subgraphs-world process) to generate

configurations in the dual NFG of ferromagnetic Ising models in an external field [9]. In a series of papers, it has also been demonstrated that, in the low-temperature regime, Monte Carlo methods for estimating the partition function of the Ising and Potts models converge faster in the dual domain than in the primal domain [10]–[15].

II. THE MODEL IN THE PRIMAL DOMAIN

Let $\mathbf{X} = (X_1, X_2, \dots, X_N)$ be a collection of random variables, each taking values in the set \mathcal{X} , which is identical to the binary field $\mathbb{Z}/2\mathbb{Z}$. The variables X_1, X_2, \dots, X_N are associated with vertices of a simple connected graph $\mathcal{G} = (\mathcal{V}, \mathcal{E})$ with $|\mathcal{V}| = N$ vertices (sites) and $|\mathcal{E}|$ edges (bonds). Two variables (X_i, X_j) interact if their corresponding vertices are connected by an edge in \mathcal{G} . An assignment of values to \mathcal{V} will be called a *configuration*, and is denoted by \mathbf{x} .

The global PMF in the primal domain is given by

$$p(\mathbf{x}) = \frac{1}{Z} \prod_{(i,j) \in \mathcal{E}} \kappa_{i,j}(x_i, x_j) \prod_{1 \leq i \leq N} \tau_i(x_i), \quad (1)$$

where Z is the normalization constant, also known as the *partition function*, factors $\kappa_{i,j}: \mathcal{X}^2 \rightarrow \mathbb{R}_{\geq 0}$ represents the pairwise potential factor, and factors $\tau_i: \mathcal{X} \rightarrow \mathbb{R}_{\geq 0}$ denotes the node potential factor.

Furthermore, we assume that pairwise potential factors have the following symmetry

$$\kappa_{i,j}(0, 0) = \kappa_{i,j}(1, 1) \quad (2)$$

$$\kappa_{i,j}(0, 1) = \kappa_{i,j}(1, 0). \quad (3)$$

Put differently, we assume that $\kappa_{i,j}(\cdot)$ is only a function of $y_{i,j} = x_i + x_j$. To lighten notations, we will denote index pair $(i, j) \in \mathcal{V}^2$ by a single index e , and express (1) as

$$p(\mathbf{x}, \mathbf{y}) = \frac{1}{Z} \prod_{e \in \mathcal{E}} \kappa_e(y_e) \prod_{1 \leq i \leq N} \tau_i(x_i), \quad (4)$$

We represent the model (i.e., the factorization (4)) by an NFG $\mathcal{G} = (\mathcal{V}, \mathcal{E})$, in which vertices represent the factors and edges represent the variables. The edge that represents some variable y_e is connected to the vertex representing the factor $\kappa_e(\cdot)$ if and only if y_e is an argument of $\kappa_e(\cdot)$. If a variable (an edge) appears in more than two factors, such a variable is replicated using an equality indicator factor. (In NFGs variables appear as arguments of one or at most of two factors.) See [2], for more details.

For a two-dimensional (2D) grid, the primal NFG of the factorization (4) is depicted in Fig. 1, where the unlabeled

boxes represent $\kappa(\cdot)$, the small unlabeled boxes represent $\tau(\cdot)$, boxes labeled “=” are instances of equality indicator factors, and boxes labeled “+” are instances of zero-sum indicator factors.

For example, in Fig. 1 the equality indicator factor involving variables x_1, x'_1 , and x''_1 is as in

$$I_{=}(x_1, x'_1, x''_1) = \delta(x_1 - x'_1) \cdot \delta(x_1 - x''_1). \quad (5)$$

Indeed $I_{=}(\cdot)$ imposes the constraint that all its incident variables are equal. The zero-sum indicator factor involving variables x_1, x_2 , and y_1 is as in

$$I_{+}(y_1, x_1, x_2) = \delta(y_1 + x_1 + x_2), \quad (6)$$

which imposes the constraint that all its incident variables sum to zero. (Recall that arithmetic manipulations are done modulo two.)

The set of variables in the primal domain includes $\mathbf{X} = \{X_i: i \in \{1, \dots, N\}\}$ and $\mathbf{Y} = \{Y_e: e \in \mathcal{E}\}$. However, these variables are not independent. Indeed, we can freely choose \mathbf{X} and therefrom fully determine \mathbf{Y} . For example, if we take \mathcal{G} to be a d -dimensional lattice, we can compute each component Y_i of \mathbf{Y} by adding two components of \mathbf{X} incident to the corresponding zero-sum indicator factor; see Fig. 1.

The number of valid configurations in the primal NFG is thus $|\mathcal{X}|^N$. The partition function of the model in (4) can be expressed as

$$Z = \sum_{\mathbf{x} \in \mathcal{X}^N} \prod_{e \in \mathcal{E}} \kappa_e(y_e) \prod_{1 \leq i \leq N} \tau_i(x_i). \quad (7)$$

A. Example: the primal Ising model

In the Ising model, each interacting pair (X_i, X_j) has an associated coupling parameter $J_{i,j}$, which measures the strength of the interaction between (X_i, X_j) . The model is called *ferromagnetic* if coupling parameters are nonnegative. The model is called *homogeneous* if coupling parameters are constant. Moreover, each site $i \in \mathcal{V}$ is under the influence of an external magnetic field represented by parameter H_i .

The energy of a configuration \mathbf{x} is given by the Hamiltonian

$$\begin{aligned} \mathcal{H}(\mathbf{x}) = & - \sum_{(i,j) \in \mathcal{E}} J_{i,j} \cdot (2\delta(x_i - x_j) - 1) \\ & - \sum_{1 \leq i \leq N} H_i \cdot (2\delta(x_i) - 1), \end{aligned} \quad (8)$$

where $\delta(\cdot)$ denotes the Kronecker delta function.¹

The probability of a configuration \mathbf{x} is given by the Boltzmann distribution

$$p_{\text{B}}(\mathbf{x}) = \frac{1}{Z} e^{-\beta \mathcal{H}(\mathbf{x})} \quad (9)$$

where $\beta \in \mathbb{R}_{\geq 0}$ denotes the inverse temperature [16].

It is straightforward to show that the Ising model can be represented via the factorization (4). Indeed, for this model $\kappa_e(\cdot)$ is given by

$$\kappa_e(y_e) = \begin{cases} e^{\beta J_e}, & \text{if } y_e = 0 \\ e^{-\beta J_e}, & \text{if } y_e = 1, \end{cases} \quad (10)$$

¹If we consider the bipolar case (i.e., if $\mathcal{X} = \{-1, +1\}$), then the Hamiltonian is $\mathcal{H}(\mathbf{x}) = - \sum_{(i,j) \in \mathcal{E}} J_{i,j} x_i x_j - \sum_{1 \leq i \leq N} H_i x_i$.

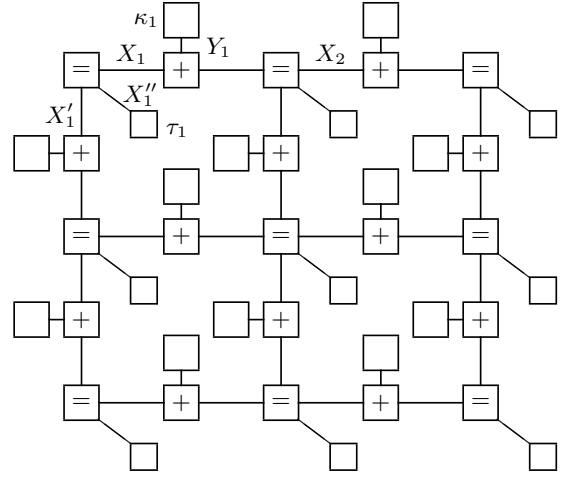


Fig. 1: Primal NFG that represents the factorization in (4). The unlabeled boxes represent $\kappa(\cdot)$, the small unlabeled boxes represent $\tau(\cdot)$, boxes labeled “=” are equality indicator factors as in (5), and boxes labeled “+” are zero-sum indicator factors given by (6). Here $Y_1 = X_1 + X_2$.

where J_e is the coupling parameter associated with edge $e \in \mathcal{E}$, and $\tau_i(\cdot)$ is as in

$$\tau_i(x_i) = \begin{cases} e^{\beta H_i}, & \text{if } x_i = 0 \\ e^{-\beta H_i}, & \text{if } x_i = 1. \end{cases} \quad (11)$$

The primal NFG of the 2D Ising model in an external field is also illustrated in Fig. 1.

III. THE MODEL IN THE DUAL DOMAIN

The dual NFG has the same topology as the primal NFG, but factors are replaced by the discrete Fourier transform (DFT) or the inverse DFT of their corresponding factors in the primal NFG. We can obtain the dual NFG of the primal NFG in Section II by replacing each factor by its one-dimensional (1D) DFT, each equality indicator factor by a zero-sum indicator factor, and each zero-sum indicator factor by an equality indicator factor. For more details, see [10], [11], [14], [15], [17].

In the dual domain, variables are denoted by the tilde symbol, which also take values in \mathcal{X} .

For $e \in \mathcal{E}$, $\tilde{\kappa}_e(\cdot)$ is given by

$$\tilde{\kappa}_e(\tilde{y}_e) = \sum_{y_e \in \mathcal{X}} \kappa_e(y_e) e^{-i2\pi y_e \tilde{y}_e / |\mathcal{X}|}. \quad (12)$$

Thus

$$\tilde{\kappa}_e(\tilde{y}_e) = \begin{cases} \kappa_e(0) + \kappa_e(1), & \text{if } \tilde{y}_e = 0 \\ \kappa_e(0) - \kappa_e(1), & \text{if } \tilde{y}_e = 1. \end{cases} \quad (13)$$

For $i \in \{1, 2, \dots, N\}$, $\tilde{\tau}_i(\cdot)$ is as in

$$\tilde{\tau}_i(\tilde{z}_i) = \frac{1}{|\mathcal{X}|} \sum_{x_i \in \mathcal{X}} \tau_i(x_i) e^{-i2\pi x_i \tilde{z}_i / |\mathcal{X}|}, \quad (14)$$

and therefore

$$\tilde{\tau}_i(\tilde{z}_i) = \begin{cases} (\tau_i(0) + \tau_i(1))/2, & \text{if } \tilde{z}_i = 0 \\ (\tau_i(0) - \tau_i(1))/2, & \text{if } \tilde{z}_i = 1. \end{cases} \quad (15)$$

For a 2D grid, the dual NFG of the model (i.e., the dual of Fig. 1) is shown in Fig. 2, where the unlabeled boxes represent $\tilde{\kappa}(\cdot)$ and the small unlabeled boxes represent $\tilde{\tau}(\cdot)$. As before, boxes labeled “=” are instances of equality indicator factors and boxes labeled “+” are instances of zero-sum indicator factors.

In the dual domain, the variables consist of $\tilde{\mathbf{Y}} = \{\tilde{Y}_e : e \in \mathcal{E}\}$ and $\tilde{\mathbf{Z}} = \{\tilde{Z}_i : i \in \{1, \dots, N\}\}$. Again, the variables $(\tilde{\mathbf{Y}}, \tilde{\mathbf{Z}})$ are not independent. We can indeed freely choose $\tilde{\mathbf{Y}}$ and therefrom fully determine $\tilde{\mathbf{Z}}$. Computing $\tilde{\mathbf{Z}}$ is easy and linear in $|\mathcal{E}|$. For example, if we take \mathcal{G} to be a d -dimensional lattice and assume periodic boundary conditions, each component \tilde{Z}_i of $\tilde{\mathbf{Z}}$ can be computed by adding $2d$ components of $\tilde{\mathbf{Y}}$ incident to the corresponding zero-sum indicator factor; see Fig. 2. The number of valid configurations in the dual NFG of the Ising model in an external field is therefore $|\mathcal{X}|^{|\mathcal{E}|}$.

If factors (13) and (15) are nonnegative, we can define the global PMF in the dual NFG as

$$p_d(\tilde{\mathbf{y}}, \tilde{\mathbf{z}}) = \frac{1}{Z_d} \prod_{e \in \mathcal{E}} \tilde{\kappa}_e(\tilde{y}_e) \prod_{1 \leq i \leq N} \tilde{\tau}_i(\tilde{z}_i). \quad (16)$$

Here Z_d denote the partition function of the dual NFG, which can be computed as

$$Z_d = \sum_{\tilde{\mathbf{y}} \in \mathcal{X}^{|\mathcal{E}|}} \prod_{e \in \mathcal{E}} \tilde{\kappa}_e(\tilde{y}_e) \prod_{1 \leq i \leq N} \tilde{\tau}_i(\tilde{z}_i). \quad (17)$$

According to the NFG duality theorem [3], the partition functions Z and Z_d are equal up to some known scale factor $\alpha(\mathcal{G})$, which depends on the topology of \mathcal{G} . With the scale factors used in (12) and (14), the NFG duality theorem states that

$$Z_d = \alpha(\mathcal{G}) \cdot Z, \quad \text{with } \alpha(\mathcal{G}) = |\mathcal{X}|^{|\mathcal{E}| - |\mathcal{V}|}. \quad (18)$$

For example, if we let \mathcal{G} be a 2D grid with periodic boundary conditions $|\mathcal{E}| = 2N$, and therefore $\alpha(\mathcal{G}) = |\mathcal{X}|^N$. For more details, see [14], [17].

A. Example: the dual Ising model

To obtain the dual NFG of an Ising model, each factor (10) is replaced by its 1D DFT as in (13), which gives

$$\tilde{\kappa}_e(\tilde{y}_e) = \begin{cases} 2 \cosh(\beta J_e), & \text{if } \tilde{y}_e = 0 \\ 2 \cosh(\beta J_e), & \text{if } \tilde{y}_e = 1. \end{cases} \quad (19)$$

Each factor (11) is replaced by its 1D DFT given by (15), therefore

$$\tilde{\tau}_i(\tilde{z}_i) = \begin{cases} \cosh(\beta H_i), & \text{if } \tilde{z}_i = 0 \\ \sinh(\beta H_i), & \text{if } \tilde{z}_i = 1. \end{cases} \quad (20)$$

Finally, each equality indicator factor is replaced by a zero-sum indicator factor and each zero-sum indicator factor by an equality indicator factor.

The dual NFG of the 2D Ising model in an external field is illustrated in Fig. 2.

Note that factors (19) are nonnegative if the model is ferromagnetic, and factors (20) are nonnegative if the model is in the presence of a nonnegative external field.

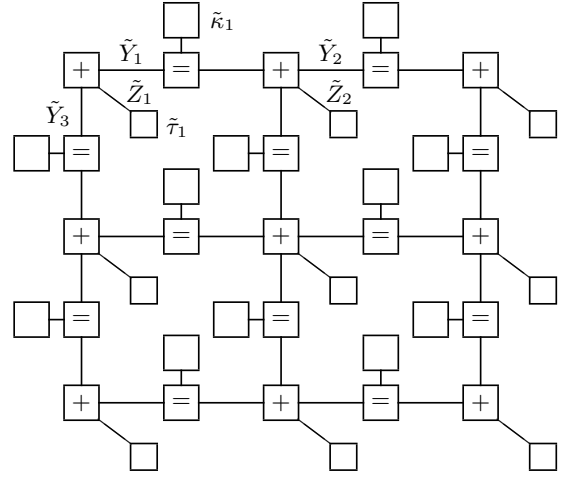


Fig. 2: Dual of the NFG in Fig. 1. The unlabeled boxes are given by (13), the small unlabeled boxes are as in (15), boxes labeled “=” are equality indicator factors, and boxes labeled “+” denote zero-sum indicator factors. Here $\tilde{Z}_2 = \tilde{Y}_1 + \tilde{Y}_2$.

IV. HIGH-TEMPERATURE SERIES EXPANSION AND THE SUBGRAPHS-WORLD PROCESS

It has been shown that the valid configurations in the dual NFG of the Ising model coincide with the terms that appear in the high-temperature series expansion of the partition function [15, Section VIII]. The equivalence holds for models with or without an external field.

The high-temperature series expansion is the basis of the polynomial randomized approximation scheme of Jerrum and Sinclair (called the subgraphs-world process) for evaluating the partition function of general ferromagnetic Ising models in a consistent external field [9].

For ferromagnetic Ising models, the process can therefore be employed to draw samples according to the global PMF of the dual NFG in (16). The samples can then be used to compute an estimate of marginal densities.

V. MARGINAL DENSITIES IN THE PRIMAL AND IN THE DUAL DOMAINS

In the primal NFG, the edge marginal PMF over $e \in \mathcal{E}$ can be computed as

$$p_{B,e}(a) = \frac{Z_e(a)}{Z}, \quad (21)$$

where $a \in \mathcal{X}$ and

$$\begin{aligned} Z_e(a) &= \sum_{\mathbf{x}} \delta(y_e - a) \prod_{e' \in \mathcal{E}} \kappa_{e'}(y_{e'}) \prod_{1 \leq i \leq N} \tau_i(x_i) \\ &= \kappa_e(a) \left(\sum_{\mathbf{x}} \delta(y_e - a) \prod_{e' \in \mathcal{E} \setminus e} \kappa_{e'}(y_{e'}) \prod_{1 \leq i \leq N} \tau_i(x_i) \right) \\ &= \kappa_e(a) S_e(a). \end{aligned} \quad (22)$$

Here, $Z_e(a) \geq 0$ and $Z = \sum_{a \in \mathcal{X}} Z_e(a) = \sum_{a \in \mathcal{X}} \kappa_e(a) S_e(a)$, hence (21) is a valid PMF over \mathcal{X} .

In coding theory terminology, the partition function Z is the dot product of the *intrinsic* message vector $\{\kappa_e(a), a \in \mathcal{X}\}$

and the *extrinsic* message vector $\{S_e(a), a \in \mathcal{X}\}$. For more details see [2].

According to sum-product message passing update rules, the edge marginal PMF vector is computed as the componentwise product of the intrinsic and extrinsic message vectors (which may be viewed as two messages going in opposite directions) up to scale. The scale factor is indeed the partition function.

In our setup, $S_e(a)$ is the partition function of an intermediate primal NFG with all factors as in Fig. 1, excluding the factor $\kappa_e(y_e)$, which should be replaced by

$$\phi_e(y_e; a) = \delta(y_e - a). \quad (23)$$

Fig. 3 (left) shows the corresponding edge in the intermediate primal NFG. The intermediate dual NFG is shown in Fig. 3 (right), in which the factor $\tilde{\kappa}_e(\tilde{y}_e)$ is replaced by

$$\tilde{\phi}_e(\tilde{y}_e; a) = \begin{cases} \delta(a) + \delta(1 - a), & \text{if } \tilde{y}_e = 0 \\ \delta(a) - \delta(1 - a), & \text{if } \tilde{y}_e = 1, \end{cases} \quad (24)$$

which is the 1D DFT of (23).

According to the NFG duality theorem (18), the partition function of the intermediate dual NFG is $\alpha(\mathcal{G}) \cdot S_e(a)$.

Similarly, in the dual NFG the edge marginal PMF over $e \in \mathcal{E}$ is given by

$$p_{d,e}(a') = \frac{\tilde{Z}_e(a')}{Z_d}, \quad (25)$$

where $a' \in \mathcal{X}$ and

$$\begin{aligned} \tilde{Z}_e(a') &= \tilde{\kappa}_e(a') \left(\sum_{\tilde{y}} \delta(\tilde{y}_e - a') \prod_{e' \in \mathcal{E} \setminus e} \tilde{\kappa}_{e'}(\tilde{y}_{e'}) \prod_{1 \leq i \leq N} \tilde{\tau}_i(\tilde{z}_i) \right) \\ &= \tilde{\kappa}_e(a') \tilde{S}_e(a'). \end{aligned} \quad (26)$$

Proposition 1. The vector $\{S_e(a), a \in \mathcal{X}\}$ and the vector $\{\tilde{S}_e(a'), a' \in \mathcal{X}\}$ are DFT pairs. \square

Proof. For $a \in \mathcal{X}$, the partition function of the intermediate dual NFG is the dot product of message vectors $\{\tilde{\phi}_e(a'; a), a' \in \mathcal{X}\}$ and $\{\tilde{S}_e(a'), a' \in \mathcal{X}\}$. Thus

$$\alpha(\mathcal{G}) \cdot S_e(a) = \sum_{a' \in \mathcal{X}} \tilde{\phi}_e(a'; a) \tilde{S}_e(a') \quad (27)$$

which gives

$$\begin{aligned} \alpha(\mathcal{G}) \cdot S_e(a) &= (\tilde{S}_e(0) + \tilde{S}_e(1)) \cdot \delta(a) \\ &\quad + (\tilde{S}_e(0) - \tilde{S}_e(1)) \cdot \delta(1 - a). \end{aligned} \quad (28)$$

After setting $a = 0$ and $a = 1$ in (28), we obtain

$$\begin{bmatrix} S_e(0) \\ S_e(1) \end{bmatrix} = \frac{1}{\alpha(\mathcal{G})} \begin{bmatrix} 1 & 1 \\ 1 & -1 \end{bmatrix} \cdot \begin{bmatrix} \tilde{S}_e(0) \\ \tilde{S}_e(1) \end{bmatrix} \quad (29)$$

as an instance of the two-point DFT transformation. \blacksquare

Proposition 2. The vector $\{p_{B,e}(a)/\kappa_e(a), a \in \mathcal{X}\}$ and the vector $\{p_{d,e}(a')/\tilde{\kappa}_e(a'), a' \in \mathcal{X}\}$ are DFT pairs. \square

Proof. From (21) and (22) we have

$$S_e(a) = Z \cdot \frac{p_{B,e}(a)}{\kappa_e(a)}, \quad a \in \mathcal{X}. \quad (30)$$

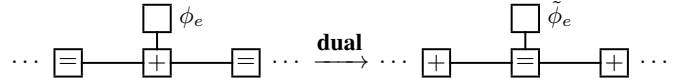


Fig. 3: An edge $e \in \mathcal{E}$ in the intermediate primal NFG (left) and in the intermediate dual NFG (right). The unlabeled box (left) is given by (23) and the unlabeled box (right) is as in (24).

Moreover (18), (25), and (26) yield

$$\tilde{S}_e(a') = Z_d \cdot \frac{p_{d,e}(a')}{\tilde{\kappa}_e(a')} \quad (31)$$

$$= \alpha(\mathcal{G}) \cdot Z \cdot \frac{p_{d,e}(a')}{\tilde{\kappa}_e(a')}, \quad a' \in \mathcal{X}. \quad (32)$$

Putting (30) and (32) in (29), and after a little rearranging, we obtain the following mapping in matrix-vector format

$$\begin{bmatrix} p_{B,e}(0)/\kappa_e(0) \\ p_{B,e}(1)/\kappa_e(1) \end{bmatrix} = \begin{bmatrix} 1 & 1 \\ 1 & -1 \end{bmatrix} \cdot \begin{bmatrix} p_{d,e}(0)/\tilde{\kappa}_e(0) \\ p_{d,e}(1)/\tilde{\kappa}_e(1) \end{bmatrix} \quad (33)$$

We conclude that the vectors $\{p_{B,e}(a)/\kappa_e(a), a \in \mathcal{X}\}$ and $\{p_{d,e}(a')/\tilde{\kappa}_e(a'), a' \in \mathcal{X}\}$ are DFT pairs. \blacksquare

By virtue of Proposition 2, it is possible to compute the edge marginal densities in one domain, and then transform them to the other domain all together. It should be emphasized that the mapping is fully local, is independent of the size of the graph N , and is independent of the topology of the interacting graph \mathcal{G} . Indeed, the relevant information regarding the rest of the graph is already incorporated in the computed edge marginal densities.

In general, estimates of marginal densities can be obtained in either domain via variational inference algorithms (e.g., the belief propagation and the tree expectation propagation algorithms) [5] or via Monte Carlo methods [6], [7], or for ferromagnetic Ising models in an external field, via the subgraphs-world process in the dual domain [9].

VI. DETAILS OF THE MAPPING FOR THE ISING MODEL

For general Ising models substituting factors (10) and (19) in (33) yields

$$\begin{bmatrix} p_{B,e}(0) \\ p_{B,e}(1) \end{bmatrix} = \begin{bmatrix} \frac{e^{\beta J_e}}{2 \cosh(\beta J_e)} & \frac{e^{\beta J_e}}{2 \sinh(\beta J_e)} \\ \frac{e^{-\beta J_e}}{2 \cosh(\beta J_e)} & \frac{e^{-\beta J_e}}{2 \sinh(\beta J_e)} \end{bmatrix} \cdot \begin{bmatrix} p_{d,e}(0) \\ p_{d,e}(1) \end{bmatrix} \quad (34)$$

which gives the inverse mapping

$$\begin{bmatrix} p_{d,e}(0) \\ p_{d,e}(1) \end{bmatrix} = \begin{bmatrix} \frac{\cosh(\beta J_e)}{e^{\beta J_e}} & \frac{\cosh(\beta J_e)}{e^{-\beta J_e}} \\ \frac{\sinh(\beta J_e)}{e^{\beta J_e}} & \frac{\sinh(\beta J_e)}{e^{-\beta J_e}} \end{bmatrix} \cdot \begin{bmatrix} p_{B,e}(0) \\ p_{B,e}(1) \end{bmatrix} \quad (35)$$

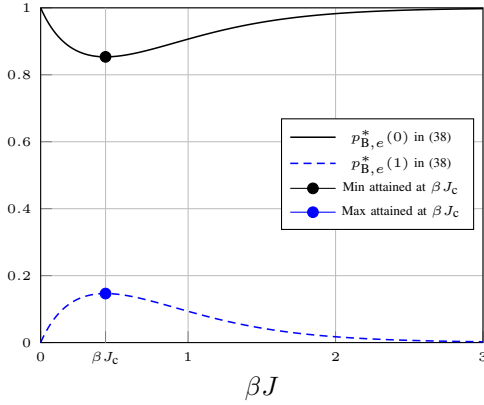


Fig. 4: The fixed points of (34) for a homogeneous and ferromagnetic Ising model as a function of βJ . The solid black line shows $p_{B,e}^*(0)$ and the dashed blue line shows $p_{B,e}^*(1)$ in (38). The circles show the fixed points at criticality of the 2D Ising model in the thermodynamic limit given by (39).

A. Sanity checks

As sanity checks, we look at the homogeneous (i.e., with constant coupling parameter J) and ferromagnetic (i.e., with $J \geq 0$) Ising model in the absence of an external field in two extreme cases, namely $\beta J \rightarrow \infty$ (i.e., the low-temperature limit) and $\beta J = 0$ (i.e., the high-temperature limit). Recall that β denotes the inverse temperature.

As $\beta J \rightarrow \infty$ the factors in the dual NFG of the model

$$\tilde{\kappa}(\tilde{y}_e) = \begin{cases} 2 \cosh(\beta J), & \text{if } \tilde{y}_e = 0 \\ 2 \sinh(\beta J), & \text{if } \tilde{y}_e = 1 \end{cases} \quad (36)$$

tend to constant factors, which implies that in the dual NFG $[p_{d,e}(0) \ p_{d,e}(1)] = [1/2 \ 1/2]$. In this case, in the primal NFG $p_{B,e}(0) = 1$ in agreement with (34).

For $\beta J = 0$, the factors in the primal NFG

$$\kappa(y_e) = \begin{cases} e^{\beta J}, & \text{if } y_e = 0 \\ e^{-\beta J}, & \text{if } y_e = 1 \end{cases} \quad (37)$$

become constant, thus $[p_{B,e}(0) \ p_{B,e}(1)] = [1/2 \ 1/2]$. In the corresponding dual NFG $p_{d,e}(0) = 1$, which is in agreement with (35).

B. Fixed points of the mapping for the Ising model

Let us again consider a homogeneous and ferromagnetic Ising model. A routine calculation shows that the fixed (invariant) points of the mapping (34) are given by

$$\begin{aligned} [p_{B,e}^*(0) \ p_{B,e}^*(1)] \\ = \begin{bmatrix} e^{\beta J} \cosh(\beta J) & e^{-\beta J} \sinh(\beta J) \\ 1 + \sinh(2\beta J) & 1 + \sinh(2\beta J) \end{bmatrix} \end{aligned} \quad (38)$$

Fig. 4 shows the fixed points (38) as a function of βJ .

Proposition 3. The minimum of $p_{B,e}^*(0)$ and the maximum of $p_{B,e}^*(1)$ are attained at the criticality of the 2D homogeneous Ising model. \square

Proof. It is well-known that in the thermodynamic limit (i.e., as $N \rightarrow \infty$) and in the absence of an external field, the

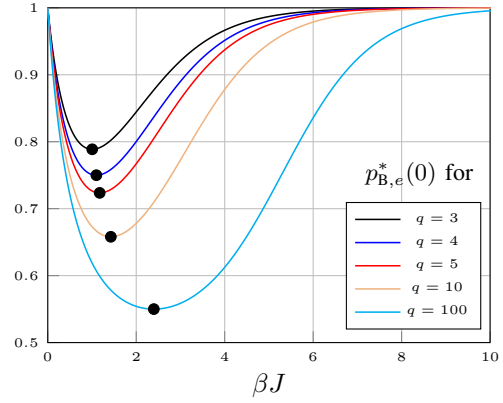


Fig. 5: The fixed points $p_{B,e}^*(0)$ in (46) for a homogeneous and ferromagnetic q -state Potts model as a function of βJ for different values of q . The circles show the fixed points at criticality of the 2D Potts model in the thermodynamic limit, which is located at $\beta J_c = \ln(1 + \sqrt{q})$.

Ising model undergoes a phase transition at the inverse critical temperature $\beta J_c = \ln(1 + \sqrt{2})/2 \approx 0.44$; see [18], [19]. A straightforward calculation shows that at criticality

$$[p_{B,e}^*(0) \ p_{B,e}^*(1)] = [(2 + \sqrt{2})/4 \ (2 - \sqrt{2})/4], \quad (39)$$

which coincides with the minimum of $p_{B,e}^*(0)$ and the maximum of $p_{B,e}^*(1)$. \blacksquare

The fixed points at criticality are illustrated by filled circles in Fig. 4. We emphasize that at criticality of the 2D homogeneous Ising model (and in the thermodynamic limit), edge marginal densities in the primal and in the dual domains are in fact equal.

VII. GENERALIZATION TO NON-BINARY MODELS

We consider the q -state Potts model to extend the mapping (33) to non-binary models. For this model, the alphabet \mathcal{X} is identical to the ring of integers modulo q , $\mathbb{Z}/q\mathbb{Z}$ for some integer $q > 2$.

In the absence of an external field, the Hamiltonian of the model is given by [19], [20]

$$\mathcal{H}(\mathbf{x}) = - \sum_{(i,j) \in \mathcal{E}} J_{i,j} \cdot \delta(x_i - x_j). \quad (40)$$

Following the same approach as in Section III, we can construct the primal NFG of the model, in which

$$\kappa_e(y_e) = \begin{cases} e^{\beta J_e}, & \text{if } y_e = 0 \\ 1, & \text{otherwise,} \end{cases} \quad (41)$$

where $y_e = x_i - x_j$ and J_e is the coupling parameter associated with $e \in \mathcal{E}$.

In the dual NFG, factors are equal to the 1D DFT of (41) given by

$$\tilde{\kappa}_e(\tilde{y}_e) = \begin{cases} e^{\beta J_e} - 1 + q, & \text{if } \tilde{y}_e = 0 \\ e^{\beta J_e} - 1, & \text{otherwise,} \end{cases} \quad (42)$$

which is nonnegative if the model is ferromagnetic (i.e., $J_e \geq 0$).

Following our approach in Section V, for the 3-state Potts model we obtain the following mapping

$$\begin{bmatrix} p_{B,e}(0)/\kappa_e(0) \\ p_{B,e}(1)/\kappa_e(1) \\ p_{B,e}(2)/\kappa_e(2) \end{bmatrix} = \begin{bmatrix} 1 & 1 & 1 \\ 1 & \omega & \omega^2 \\ 1 & \omega^2 & \omega^4 \end{bmatrix} \cdot \begin{bmatrix} p_{d,e}(0)/\tilde{\kappa}_e(0) \\ p_{d,e}(1)/\tilde{\kappa}_e(1) \\ p_{d,e}(2)/\tilde{\kappa}_e(2) \end{bmatrix} \quad (43)$$

where $\omega = e^{-2\pi i/3}$ and $i = \sqrt{-1}$.

Due to the symmetry in the factors (42), $p_{d,e}(1)/\tilde{\kappa}_e(1)$ and $p_{d,e}(2)/\tilde{\kappa}_e(2)$ are equal. Thus from (43) we obtain

$$\frac{p_{B,e}(1)}{\kappa_e(1)} = \frac{p_{d,e}(0)}{\tilde{\kappa}_e(0)} - \frac{1}{2} \left(\frac{p_{d,e}(1)}{\tilde{\kappa}_e(1)} + \frac{p_{d,e}(2)}{\tilde{\kappa}_e(2)} \right) \quad (44)$$

$$= \frac{p_{d,e}(0)}{\tilde{\kappa}_e(0)} - \frac{p_{d,e}(1)}{\tilde{\kappa}_e(1)}, \quad (45)$$

and analogously for $p_{B,e}(2)/\kappa_e(2)$.

For an arbitrary q , the mapping can be represented via the q -point DFT matrix, i.e., the Vandermonde matrix for the roots of unity [21]. It is easy to show that for homogeneous and ferromagnetic q -state Potts models, the minimum of $p_{B,e}^*(0)$ and the maximum of $p_{B,e}^*(1)$ are also attained at the criticality of the 2D Potts model in the thermodynamic limit. The criticality is located at $\beta J_c = \ln(1 + \sqrt{q})$; see [20].

The fixed points of the mapping are given by

$$p_{B,e}^*(0) = \frac{e^{\beta J}(e^{\beta J} + q - 1)}{e^{2\beta J} + 2(q-1)e^{\beta J} - q + 1} \quad (46)$$

and

$$p_{B,e}^*(t) = \frac{e^{\beta J} - 1}{e^{2\beta J} + 2(q-1)e^{\beta J} - q + 1}. \quad (47)$$

At criticality βJ_c , we obtain

$$p_{B,e}^*(0) = \frac{1}{2} \left(1 + \frac{1}{\sqrt{q}} \right) \quad (48)$$

and

$$p_{B,e}^*(t) = \frac{1}{2(q-1)} \left(1 - \frac{1}{\sqrt{q}} \right), \quad (49)$$

for $t \in \{1, 2, \dots, q-1\}$.

The fixed points in (46) and (47) are shown in Figs. 5 and 6, where the filled circles show the fixed points at criticality of the 2D Potts model. Like the Ising model, the minimum of $p_{B,e}^*(0)$ and the maximum of $p_{B,e}^*(1)$ are attained at the criticality of the 2D homogeneous Potts model (without an external field) and in the thermodynamic limit.

Finally note that in the many-component limit $q \rightarrow \infty$, we have

$$\lim_{q \rightarrow \infty} p_{B,e}^*(0) = \frac{1}{2}. \quad (50)$$

VIII. GENERAL BINARY PAIRWISE MARKOV RANDOM FIELDS

In our analysis of the Ising model, we exploited the symmetry in the factors as $\kappa_{(i,j)}(x_i, x_j)$ could be expressed as $\kappa_e(y_e)$, where $y_e = x_i + x_j$ and e denoted the edge (i, j) .

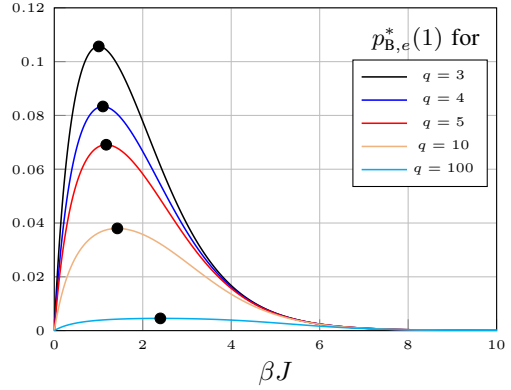


Fig. 6: Everything as in Fig. 5 but for $p_{B,e}^*(1)$ in (47).

If there is no such symmetry in the factors, marginal densities in primal and in dual domains are related via the following mapping

$$\begin{bmatrix} p_{B,(i,j)}(0,0)/\kappa_{(i,j)}(0,0) \\ p_{B,(i,j)}(1,0)/\kappa_{(i,j)}(1,0) \\ p_{B,(i,j)}(0,1)/\kappa_{(i,j)}(0,1) \\ p_{B,(i,j)}(1,1)/\kappa_{(i,j)}(1,1) \end{bmatrix} = \begin{bmatrix} W & W \\ W & -W \end{bmatrix} \cdot \begin{bmatrix} p_{d,(i,j)}(0,0)/\tilde{\kappa}_{(i,j)}(0,0) \\ p_{d,(i,j)}(1,0)/\tilde{\kappa}_{(i,j)}(1,0) \\ p_{d,(i,j)}(0,1)/\tilde{\kappa}_{(i,j)}(0,1) \\ p_{d,(i,j)}(1,1)/\tilde{\kappa}_{(i,j)}(1,1) \end{bmatrix} \quad (51)$$

where the matrix

$$\begin{bmatrix} W & W \\ W & -W \end{bmatrix}$$

is a block matrix with components $W = \begin{bmatrix} 1 & 1 \\ 1 & -1 \end{bmatrix}$.

Alternatively, the transformation (51) can be expressed via the Kronecker product $W \otimes W$. It is then straightforward to generalize the mapping to higher-order Markov random fields.

In this setup, the factor $\tilde{\kappa}_{(i,j)}(\cdot)$ is the 2D DFT of $\kappa_{(i,j)}(\cdot)$. Indeed, $\tilde{\kappa}_{(i,j)}(0,0)$ is the DC sum, which is equal to

$$\begin{aligned} \tilde{\kappa}_{(i,j)}(0,0) &= \kappa_{(i,j)}(0,0) + \kappa_{(i,j)}(1,0) + \kappa_{(i,j)}(0,1) + \kappa_{(i,j)}(1,1). \end{aligned}$$

In the (binary) Ising model, there is symmetry in the pairwise potential factors. The symmetry allows us to write the mapping between edge marginal densities $p_{B,e}(\cdot)$ and $p_{d,e}(\cdot)$ via the 2×2 matrix W as in (33).

ACKNOWLEDGMENTS

The author is grateful to G. David Forney for his continued support and his constructive comments on an earlier draft of this paper. The author also wishes to acknowledge helpful discussions with Justin Dauwels.

REFERENCES

- [1] M. Luby and P. Dagum, "Approximating probabilistic inference in Bayesian belief networks is NP-hard," *Artificial Intelligence*, vol. 60, pp. 141–153, March 1993.
- [2] G. D. Forney, Jr., "Codes on graphs: normal realizations," *IEEE Trans. Inf. Theory*, vol. 47, pp. 520–548, Feb. 2001.
- [3] A. Al-Bashabsheh and Y. Mao, "Normal factor graphs and holographic transformations," *IEEE Trans. Inf. Theory*, vol. 57, pp. 752–763, Feb. 2011.
- [4] G. D. Forney, Jr., "Codes on graphs: duality and MacWilliams identities," *IEEE Trans. Inf. Theory*, vol. 57, pp. 1382–1397, Feb. 2011.
- [5] K. P. Murphy, *Machine Learning: A Probabilistic Perspective*. MIT Press, 2012.
- [6] A. E. Gelfand and A. F. Smith, "Sampling-based approaches to calculating marginal densities," *Journal of the American Statistical Association*, vol. 85, pp. 398–409, 1990.
- [7] C. Robert and G. Casella, *Monte Carlo Statistical Methods*. Springer-Verlag, 2004.
- [8] K. Binder and D. W. Heermann, *Monte Carlo Simulation in Statistical Physics*. Springer, 2010.
- [9] M. Jerrum and A. Sinclair, "Polynomial-time approximation algorithms for the Ising model," *SIAM Journal on Computing*, vol. 11, pp. 1087–1116, Oct. 1993.
- [10] M. Molkaraie and H.-A. Loeliger, "Partition function of the Ising model via factor graph duality," *Proc. 2013 IEEE Int. Symp. on Inf. Theory*, Istanbul, Turkey, July 7–12, 2013, pp. 2304–2308.
- [11] A. Al-Bashabsheh and Y. Mao, "On stochastic estimation of the partition function," *Proc. 2014 IEEE Int. Symp. on Inf. Theory*, Honolulu, USA, June 29 – July 4, 2014, pp. 1504–1508.
- [12] M. Molkaraie, "An importance sampling scheme for models in a strong external field," *Proc. 2015 IEEE Int. Symp. on Inf. Theory*, Hong Kong, June 14–19, 2015, pp. 1179–1183.
- [13] M. Molkaraie, "An importance sampling algorithm for the Ising model with strong couplings," *Proc. 2016 Int. Zurich Seminar on Communications (IZS)*, Zurich, Switzerland, March 2–4, 2016, pp. 180–184.
- [14] M. Molkaraie, "The primal versus the dual Ising model," *Proc. 55th Annual Allerton Conf. on Communication, Control, and Computing*, Monticello, USA, Oct. 3–6, 2017, pp. 53–60.
- [15] M. Molkaraie and V. Gómez, "Monte Carlo methods for the ferromagnetic Potts model using factor graph duality," *IEEE Trans. Inf. Theory*, vol. 64, pp. 7449–7464, Dec. 2018.
- [16] J. M. Yeomans, *Statistical Mechanics of Phase Transitions*. Oxford University Press, 1992.
- [17] G. D. Forney, Jr., "Codes on graphs: Models for elementary algebraic topology and statistical physics," *IEEE Trans. Inf. Theory*, vol. 64, pp. 7465–7487, Dec. 2018.
- [18] L. Onsager, "Crystal statistics. I. A two-dimensional model with an order-disorder transition," *Phys. Rev.*, vol. 65, pp. 117–149, Feb. 1944.
- [19] R. J. Baxter, *Exactly Solved Models in Statistical Mechanics*. Dover Publications, 2007.
- [20] F. Y. Wu, "The Potts model," *Rev. of Modern Phys.*, vol. 54, pp. 235–268, Jan. 1982.
- [21] R. N. Bracewell and R. N. Bracewell, *The Fourier Transform and Its Applications*. McGraw-Hill, 1986.